Title

Characterization of A Novel Mouse Model of Arrhythmogenic Right Ventricular Cardiomyopathy Harboring Plakophilin-2 Patient Genetics

Author

Mataraarachchi, Nirosh Eranga

Publication Date

2020

Peer reviewed|Thesis/dissertation

UNIVERSITY OF CALIFORNIA SAN DIEGO

Characterization of A Novel Mouse Model of Arrhythmogenic Right Ventricular Cardiomyopathy Harboring Plakophilin-2 Patient Genetics

A thesis submitted in partial satisfaction of the
requirements for the degree Master of Science

in

Biology

by

Nirosh Eranga Mataraarachchi

Committee in charge:

Professor Farah Sheikh, Chair
Professor Deborah Yelon, Co-Chair
Professor Amy Kiger

2020

The thesis of Nirosh Eranga Mataraarachchi is approved, and it is acceptable in quality and form for publication on microfilm and electronically:

_____

_____

Co-Chair

_____

Chair

University of California San Diego

2020

Table of Contents

Dedication

To both my parents, who came to the United States of America with no education and little English in hopes of providing a future filled with possibilities and happiness for myself and my younger sister; to my mother, who is the hardest working person I know, who will continue to do anything for her children even after working more than eleven hours in a day for five days a week; to my father, who has wanted to provide the best for us when he knew it was not possible; to my friends, who have supported me and wished the genuine best for me in all my pursuits and passions. I dedicate this thesis to my supporters, without whom nothing would be possible.

List of Abbreviations

AAV	Adeno-associated virus
α-Cat	Alpha-catenin
ANF	Atrial natriuretic factor
ARVC	Arrhythmogenic right ventricular cardiomyopathy
β-Cat	Beta-catenin
BNP	B-type natriuretic factor
BW	Body weight
Cas9	CRISPR associated protein 9
crRNA	CRISPR RNA
Col1a1	collagen 1 types I
Col3a1	collagen 1 types III
CRISPR	clustered regularly interspaced short palindromic repeats
Cx43	Connexin-43
DSC2	Desmocolin-2
DSG2	Desmoglein-2
DSP	Desmoplakin
ECG	Electrocardiogram
FP	Field potential
GAPDH	Glyceraldehyde 3-Phosphate Dehydrogenase
Hom	Homozygous
HW	Heart weight
IACUC	Institutional Animal Care and Use Committee
ICD	Intercalated discs
JUP	Plakoglobin
LV	Left ventricle
MRI	Magnetic resonance imaging
N-Cad	N-cadherin
P1	Postnatal day 1
PBS	Phosphate-buffered saline
PCR	Polymerase chain reaction
PKP2	Plakophilin-2
qPCR	Quantitative PCR
RT-qPCR	Reverse transcription-quantitative polymerase chain reaction
RV	Right ventricle
SERCA2	Sarcoplasmic Reticulum Calcium ATPase
SCD	Sudden cardiac death

List of Tables and Figures

Acknowledgments

First and foremost, I would like to acknowledge and thank Professor Farah Sheikh for her overwhelming support and dedication to my studies as a student in her laboratory. Her mentorship and guidance has not only influenced me as a scientist, but has also helped me as a person. She has shown me the beauty between rigor and simplicity. Secondly, I would like to acknowledge and thank Mr. William Hank Bradford for being an extraordinary graduate student mentor. Hank's work ethic and diligence motivates me to be a better and more thorough scientist every day. He has been a beacon of support, guidance, and friendship. I am extremely grateful for all the care, praise, criticism, and encouragement Hank has given me throughout my time as a student in the Sheikh laboratory. Further, I would like to acknowledge all members of the Sheikh laboratory for their support and help in both directly or indirectly supporting this project: Dr. Kyohei Fujita, Dr. Yan Liang, Dr. Jie Wang, Dr. Jing Zhang, and Arryane Do.

Vita

2018-2021	Teaching Assistant, University of California San Diego
2019	Phi Beta Kappa
2019	Summa Cum Laude
2019	Bachelor of Science (Distinction), University of California San Diego
2019	BrightSpinnaker Diversity Fellowship
2020	Master of Science, University of California San Diego

Abstract of the Thesis

Characterization of A Novel Mouse Model of Arrhythmogenic Right Ventricular Cardiomyopathy Harboring Plakophilin-2 Patient Genetics

by

Nirosh Eranga Mataraarachchi

Master of Science

in

Biology

University of California San Diego, 2020

Professor Farah Sheikh, Chair

Professor Deborah Yelon, Co-Chair

Arrhythmogenic right ventricular cardiomyopathy (ARVC) is a genetic cardiac disease and a leading cause of sudden cardiac death (SCD) in young athletes, often triggered by exercise (adrenergic stress). Through genetic studies, 40% of ARVC patients have mutations within desmosomal genes, a mechanical junction that helps anchor cells together. Plakophilin-2

(PKP2) is the most mutated desmosomal gene; however, there are limited insights on underlying mechanisms that drive ARVC due to PKP2 patient genetics.

In my studies, I have characterized a newly generated knockin mouse model that harbors a prevalent human PKP2 splice site mutation (c.2146-1G>C) that we show recapitulates the full spectrum of ARVC in mice. PKP2 Homozygous (Hom) mutant mice are viable at birth but exhibit SCD starting at 4 weeks, while encompassing full disease features of ARVC. I hypothesized that neonatal PKP2 Hom mutant mice will represent a stage where early ARVC disease features are observed in the absence of overt structural disease.

My thesis studies have shown that neonatal PKP2 Hom mutant hearts do not exhibit significant differences in (i) gross morphology as evidenced by similar heart weight to body weight ratios to controls and (ii) gene expression of cardiac stress markers and pro-fibrotic genes when compared to controls. However, upon protein blot analysis, I discovered neonatal PKP2 mutant cardiomyocytes harbored a larger molecular weight PKP2 mutant protein, in the absence of endogenous PKP2 alongside specific loss of desmosomal junctional proteins (desmoplakin, desmoglein-2) when compared to controls. These defects were observed in the absence of effects on other mechanical junction (fascia adherens junction) genes as evidenced by intact localization of N-cadherin. Furthermore, I observed baseline arrhythmias in neonatal PKP2 Hom mutant cardiomyocytes, which are reminiscent of the early electrical dysfunction seen in ARVC patients, in the absence of overt structural disease. In conclusion, my thesis studies have identified a stage in our PKP2 Hom mutant model that will help define early disease driving

pathways, thus providing insights into mechanisms driving electrical dysfunction and SCD in ARVC.

Chapter 1

Introduction

1.1 Genetic Heart Disease

Heart disease is the most common cause of death in the world. In 2016, close to 18 million people died from cardiovascular disease (WHO Report). There have been numerous associated risk factors for cardiac disease such as high cholesterol, high blood pressure, metabolic syndromes, and genetics (Mozaffarian Dariush et al. 2016). Genetic factors are recognized as one of the leading risk factors (Kathiresan and Srivastava 2012; Mozaffarian Dariush et al. 2016). Analysis of inherent human mutations can reveal underlying mechanisms behind human genetic cardiac disease. An understanding of how these mechanisms manifest in cardiac disease will allow for the identification of novel therapeutic targets. Extensive research has identified a direct association between genetic mutations and cardiac disease. There have been specific pathogenic mutations identified for a wide spectrum of cardiac diseases affecting cardiac arrhythmias and cardiac function (Carrier et al. 2015; Yadav et al. 2019; Zhang et al. 2018). Arrhythmogenic right ventricular cardiomyopathy (ARVC) is a genetic cardiac disease with broad disease manifestations, which include arrhythmogenic deficiencies, ventricular dysfunction and heart failure (Sen-Chowdhry et al. 2010). Human genetic studies have also linked mutations within components of the cardiac desmosome to ARVC, thus terming it a "disease of the desmosome" (Marcus, Edson, and Towbin 2013; Sen-Chowdhry et al. 2010). Studying how dysfunction of the cardiac desmosome contributes to ARVC's wide spectrum of disease will broadly shed light on underlying mechanisms contributing to various cardiac diseases.

1.2 Clinical features of ARVC

ARVC encompasses a wide spectrum of cardiac disease features that manifests as both structural and electrical defects. The prevalence of ARVC is 1 in 5000 people and it accounts for up to 10% of deaths in young populations in the < 65 age group (Sen-Chowdhry et al. 2010; Tabib et al. 2003). Amongst these, premature sudden death occurs in individuals 35 years and under (Cho 2018). However, these numbers may be inaccurate and more detrimental due to misdiagnoses and poor diagnostic markers (Sen-Chowdhry et al. 2010; Tabib et al. 2003). ARVC was originally discovered as a right ventricular (RV) dominant disease. However, recent studies have shown evidence of patients with left ventricular (LV) dominant and bi-ventricular dysfunction (Sen-Chowdhry et al. 2010). Ventricular dysfunction, fibrofatty replacement, and ventricular arrhythmias are all clinical manifestations found in patients and causes of sudden death (Sen-Chowdhry et al. 2010). ARVC is one of the leading causes of sudden death, especially amongst young athletes (Sen-Chowdhry et al. 2010). Exercise (adrenergic stress), specifically, has been found to increase ventricular arrhythmias and risk of sudden death (Corrado et al. 2003). During the "concealed" phase of ARVC, sudden death, which are caused by the lethal arrhythmias, is often the first manifestation of ARVC (Dalal et al. 2005). Structural deficits are also important in ARVC, as some hearts from ARVC patients exhibit fibro-fatty replacement ensuing in ventricular remodeling, which is triggered by cardiomyocyte death and an inflammatory response (Dalal et al. 2005). Heterogeneity exists within ARVC disease features between patients as well. Some patients exhibit purely electrical dysfunction as indicated by cardiac arrhythmias alone, while others exhibit overt structural defects as indicated by cardiac arrhythmias alongside ventricular dysfunction and/or fibrofatty replacement (Dalal et al. 2005). Human genetic studies have identified that a major cause for why ARVC patients manifest these

particular clinical features has been linked to the disruption of the cardiac desmosome (Sen-Chowdhry et al. 2010).

1.3 Cardiac ICD/Desmosome

The desmosome is a specialized cell-cell junction that acts to mechanically anchor adjacent cells (Thiene, Corrado, and Basso 2007). Desmosomes are found within intercalated disc (ICD), which are cell-cell adhesion structures that connect cardiac muscle cells, or cardiomyocytes, together (Sheikh, Ross, and Chen 2009). ICD are composed of the desmosome, fascia adherens and gap junctions (Sheikh, Ross, and Chen 2009). The cardiac desmosome is composed of desmoplakin (DSP), desmocolin-2 (DSC2), desmoglein-2 (DSG2), plakoglobin (JUP), and plakophilin-2 (PKP2). These desmosomal proteins have distinct structural domains and features that collectively help anchor cell membranes to the intermediate filament network in cardiomyocytes. DSG2 and DSC2, known as desmosomal cadherins, are transmembrane proteins that form calcium-dependent heterophilic cell-cell adhesive interactions. JUP and PKP2 are cytoplasmic cadherin binding partners (armadillo proteins) that signal and regulate cadherin adhesive activity. DSP is a plakin protein that links the cadherins to the intermediate filament network, composed of desmin in the cardiomyocytes (Sheikh, Ross, and Chen 2009). Critical proteins found within the fascia adherens junctions include N-cadherin (N-Cad), beta-catenin (β-Cat), alpha-catenin (α-Cat), and JUP, while connexin-43 (Cx43) is a component of the gap junction. The desmosome and fascia adherens are two cell-cell junction components important for maintaining mechanical integrity between cells whereas gap junctions are important for electrical coupling across cells (Sheikh, Ross, and Chen 2009).

1.4 Genetics of ARVC: PKP2 is the Most Frequently Mutated Desmosomal Gene

Human genetic studies highlight that 40% of mutations found in ARVC patients are present within desmosomal genes (Sen-Chowdhry et al. 2010). Of those mutations, over 70% of desmosomal mutations are found in the PKP2 gene (Sen-Chowdhry et al. 2010). Most ARVC-associated desmosomal gene mutations are autosomal dominant; however, there has also been evidence of recessive mutations (Norgett et al. 2000; Ohno 2016). DSP was the first desmosomal gene linked to autosomal dominant ARVC and mutations within the DSP gene have been implicated in both left-dominant and bi-ventricular ARVC (Rampazzo et al. 2002; Te Riele et al. 2012). Recessive mutations in the JUP and DSP genes have also been linked to cardiocutaneous diseases, thus highlighting the significance of desmosomal defects in connection to not only the heart but also skin (Carvajal-Huerta 1998; Simpson et al. 2009). In order to dissect the impact of specific genetic alterations in human disease, animal models have been of essential importance.

1.5 Mouse Models: Limitations to Understanding How Human PKP2 Genetics Drive ARVC

Animals model have been crucial to recapitulating disease progression and dissecting mechanisms underlying human genetic based diseases. Various genome engineering techniques such as clustered regularly interspaced short palindromic repeats (CRISPR)/CRISPR associated protein 9 (Cas9) to knockin gene mutations or knockout genes, and silencing short hairpin RNA (shRNA) and morpholinos, have been exploited to genetically alter many species such as mice, rats, zebrafish, pigs and primates (Baumgart and Beyer 2017). Mice, however, have become the preferred animal species to model cardiac diseases in the last quarter century. Humans and mice share a large percentage of genomic information as close to 99% of mouse genes have a human homologue and 96% of homologues lie within a similar conserved syntenic interval (DeBry and

Seldin 1996). Additionally, many mouse models have been able to recapitulate various aspects of genetic cardiac disease. However, there are limited animal models exploiting human PKP2 mutant genetics to determine their sufficiency in driving ARVC. Initial studies exploited a conventional global PKP2 gene knockout strategy, which resulted in embryonic lethality at day 11.5, showing a requirement for PKP2 in early cardiac development (Grossmann et al. 2004). Subsequent studies exploited PKP2 heterozygous knockout mice and revealed baseline arrhythmias in mice. However, contractile dysfunction, fibro-fatty replacement of the myocardium, and sudden death were not observed (Cerrone et al. 2012). Recent studies have utilized a cardiac-inducible PKP2 knockout strategy (adult heart), which resulted in ventricular dysfunction, sudden death and fibrosis in mice; however, electrical defects were only present under isoproterenol stress (Cerrone et al. 2017). In addition to the lack of baseline arrhythmias, fatty replacement could not be observed in hearts of adult cardiac-specific PKP2 deficient mice (Cerrone et al. 2017). Several studies have overexpressed PKP2 mutations in mice *in vivo* using adeno-associated viral (AAV) strategies. Cardiac-specific AAV-mediated overexpression of the PKP2 R735X mutation in mice resulted in an exercise-dependent ARVC phenotype (Cruz et al. 2015). Endurance exercise training of these mice resulted in RV dysfunction, observed as impaired global RV systolic function and RV regional wall motion abnormalities, thus encompassing the ventricular deficits associated with ARVC (Cruz et al. 2015). Additionally, these endurance-trained mice displayed Cx43 loss, which was thought to drive the altered electrical activity. Stable cardiac expression of this PKP2 mutant could only be achieved after 4 weeks of AAV9-R735X treatment (Cruz et al. 2015), highlighting the exclusive impact of this PKP2 mutant in the adult heart. Transgene approaches have also been utilized to better understand PKP2 mutations. Cardiac-specific overexpression of truncated S329X PKP2 mutation

provided similar insights into the structural and electrical defects seen in ARVC patients (Moncayo-Arlandi et al. 2016). PKP2 S329X mutant transgenic mice experienced significant QRS elongation, thus encompassing the arrhythmias seen in ARVC patients. However, a high transgene expression as well as 7 months of aging were required for arrhythmias to appear (Moncayo-Arlandi et al. 2016). In addition, the classic features of ARVC such as fibrofatty replacement of cardiac muscle and sudden death could not be observed in this PKP2 mutant mouse model (Moncayo-Arlandi et al. 2016). ARVC patients, however, harbor PKP2 mutations globally (in all tissues) and at all developmental stages, thus, developing animal models where PKP2 mutations are globally present in all tissues and at all development stages would more closely recapitulate the human condition.

1.6 RNA Splicing

Evidence suggests that altered RNA splicing may be a critical mechanism through which PKP2 genetics drives ARVC (Gerull et al. 2004; Groeneweg et al. 2014). Approximately one third of all disease-causing mutations are caused by defects in RNA splicing (Lim et al. 2011). Genetic diseases such as Charcot-Marie-Tooth disease and Fabry disease have been classified as RNA splicing related diseases as mutations were shown to disrupt splicing at the canonical splice acceptor sites located at the 3' end of introns (Anna and Monika 2018; Guernsey et al. 2010; Watanabe et al. 2013). Disruption of splice acceptor sites can have multiple consequences resulting in either premature termination, intron retention, or exon skipping (Guernsey et al. 2010; Watanabe et al. 2013). The Sheikh's lab assessment of the Genome Aggregation Database has revealed canonical splice acceptor site variants within all five human desmosomal genes (PKP2, DSP, JUP, DSG2, DSC2) (**Table 1**), altogether highlighting the importance of testing the

relevance of RNA splicing as a mechanism underlying ARVC. However, no models exist to give insight into the role of altered RNA splicing as a trigger for ARVC. By generating a mouse model harboring a prevalent PKP2 RNA splice site mutation, we will have the potential to determine the sufficiency of RNA splicing to contribute to ARVC disease pathogenesis.

1.7 Rationale, Aim, and Hypothesis

ARVC is a genetic cardiac disease characterized by early ventricular arrhythmias, progressing into ventricular dysfunction and heart failure, as marked by increased ventricular filling volumes and reduced function, as well as structural defects including fibrofatty replacement of the myocardium indicated by the presence of fatty and fibrotic tissue replacing healthy tissue, leading to sudden death (Sen-Chowdhry et al. 2010). Early detection is hindered as the clinical symptoms of ARVC have not yet developed (often observed as a structurally normal heart) in the concealed phase, yet they are still at risk for sudden death, especially during strenuous exercise (Dalal et al. 2005). Evidence has additionally shown heterogeneity within ARVC disease features. Some patients exhibit purely electrical dysfunction as indicated by cardiac arrhythmias alone, while others exhibit overt structural defects as indicated by cardiac arrhythmias alongside ventricular dysfunction and/or fibrofatty replacement (Dalal et al. 2005). Human genetic studies have highlighted that 40% of ARVC patients carry mutations within desmosomal genes, which encode mechanical cell-cell junction proteins that helps anchor cells together (Sen-Chowdhry et al. 2010). Thus, ARVC is termed a cardiac "disease of the desmosome". Over 70% of desmosomal gene mutations linked to human ARVC occur within the PKP2 gene (Sen-Chowdhry et al. 2010). PKP2 is critical to the proper functioning of the desmosome as a member of the plakin superfamily (Vermij, Abriel, and van Veen 2017). PKP2

functions to link desmosomal cadherins to DSP, which then tether the intermediate filaments in the cardiac cytoskeleton and thus, make it necessary for normal localization of DSP to desmosomes (Bass-Zubek et al. 2008). However, there are limited mouse models that recapitulate PKP2 genetics to determine their sufficiency in driving ARVC disease features. Recent evidence highlights that altered RNA splicing may be a mechanism by which PKP2 genetics drives ARVC (Gerull et al. 2004; Groeneweg et al. 2014); however, no models exist to determine whether RNA splicing mutations are triggers for ARVC, especially in early disease. By creating a novel PKP2 mutant mouse model harboring a prevalent PKP2 splicing mutation (c.2146-1G>C) in ARVC populations (Gerull et al. 2004; Svensson et al. 2016; Syrris et al. 2006), we aim to determine the sufficiency of PKP2 RNA splicing alterations to drive classic early and late cardiomyocyte disease features associated with ARVC, and provide a novel platform to mine for early mechanisms and therapeutics for ARVC.

Hypothesis:

Altered PKP2 RNA splicing is sufficient to drive ARVC and neonatal PKP2 mutant mice will represent a stage where early ARVC disease features are observed in the absence of overt structural disease.

Table 1: Compilation of RNA splice acceptor site mutations in the five classic desmosomal genes (gnomAD) and reported associations with ARVD/C disease pathogenesis (ClinVar) (Bradford WH., Unpublished Data, 2020).

Desmosomal Gene	Variant	Pathogenic?
PKP2	c.1379-1G>A	Conflicting
	c.1511-1G>T	Yes
	c.1511-2A>T	Yes
	c.1689-1G>C	Likely
	c.2146-1G>C	Yes
	c.2490-47 (del)	Unknown
DSP	c.598-2A>C	Unknown
	c.598-2A>G	Unknown
	c.598-1G>C	Unknown
	c.1141-2A>G	Yes
	c.2131-3 (del)	Unknown
	c.2298-1G>C	Unknown
	c.3085-1G>A	Unknown
JUP	c.910-1G>C	Unknown
	c.993-1G>T	Unknown
DSG2	c.82-1G>A	Unknown
	c.379-1G>C	Unknown
	c.1424-1G>T	Unknown
	c.1652-1G>A	Likely
	c.2002-2A>G	Unknown
DSC2	c.631-2A>G	Likely
	c.1664-1G>C	Unknown

Chapter 2

Materials and Methods

2.1 Mouse Model

The PKP2 IVS10-1G>C knock-in mouse model was previously generated and validated by the Sheikh Laboratory. Briefly, PKP2 c.2146-1G>C equivalent knock-in mice were generated via co-injection of Cas9 protein, PKP2 mutation site-specific CRISPR RNA (crRNA), trans-activating crRNA (*S. pyogenes*), and PKP2 c.2146-1G>C single-strand oligodeoxynucleotide (sequence not shown) into pronuclei of C57BL/6 mouse zygotes, using methods previously described (Bass-Zubek et al. 2008). PCR analysis on tail DNA using mutation specific primers (forward, CAGGATGTGTCTCACAACAC; reverse, AGAATGCACCTATGGCTTGC) and sequencing were used to identify PKP2 c.2146-1G>C heterozygous knock-in mice. Knock-in mice were backcrossed with C57BL/6 mice for at least three generations to reduce off-target effects. Heterozygous PKP2 IVS10-1G>C knock-in mice were inbred to generate sufficient control and homozygous PKP2 IVS10-1G>C knock-in mice for studies. All animal procedures were in full compliance with the guidelines approved by the University of California-San Diego Institutional Animal Care and Use Committee (IACUC) and carried out in accordance with the Guide for the Care and Use of Laboratory Animals of the National Institutes of Health.

2.2 Reverse Transcription-quantitative PCR (RT-qPCR)

Total RNA was extracted from postnatal day 1 mouse heart ventricles using TRIzol (Invitrogen). After RNA isolation, genomic DNA elimination and reverse transcription were performed following PrimeScript RT reagent Kit with gDNA Eraser procedures (Takara). Quantitative PCR (qPCR) was performed using standard two-step SYBR green qPCR procedures. Primers specific for PKP2 exons 11-13 (E11-13)- (forward, GCACGAGACCTTCTGAACAC, reverse, GCAGTCCGGCTGTTGACAAA), cardiac stress

markers (atrial natriuretic factor (ANF) primers– (forward, GATAGATGAAGGCAGGAAGCCGC; reverse, AGGATTGGAGCCCAGAGTGGACTAGG), B-type natriuretic factor (BNP) primers –(forward, TGTTTCTGCTTTTCCTTTATCTGTC; reverse, BCTCCGACTTTTCTC TTATCAGCTC) and profibrotic/collagen genes, collagen α1 type I (Col1a1) primers –(forward, TCACCAAACTCAGAAGATGTAGGA, reverse, CTCCGACTTTTCTCTTATCAGCTC), and collagen α1 type 3 (Col1a3) primer – (forward, ACAGCAGTCCAACGTAGATGAAT, reverse, TCACAGATTATGTCATCGCAAAG) using standard procedures.

2.3 Surface Electrocardiogram

Four week old mice were anesthetized with 1% isoflurane. Needle electrodes (30 gauge) were inserted subcutaneously into right forearm and left leg. ECG signals were amplified using Warner Instruments DP-304 Differential Amplifier bandpass filtered between 0.1 and 100 Hz. Signal was further filtered through a Quest Scientific HumBug 50/60 Hz Noise Eliminator and digitized at 3000 Hz.

2.4 Magnetic Resonance (MR) Imaging

In vivo MR cardiac imaging was performed on a 7T horizontal bore MR scanner. Five week old mice were anesthetized at 1-2% isoflurane for the scan. A quadrature volume coil was used to transmit RF signal and a surface coil was used to receive RF signal. IntraGate was used to perform retrospective gating on the cardiac cycle in mice. Analysis methods were previously described (Lyon et al. 2014).

2.5 Histological Analysis

Hearts from 6 week old mice were perfused in relaxation buffer consisting of 100 mM KCl in phosphate-buffered saline (PBS) followed by perfusion fixation with 4% paraformaldehyde solution. For assessment of cardiac fibrosis and collagen deposition, hearts were embedded in paraffin and whole-heart sections were stained with Masson's trichrome (Sigma-Aldrich) according to manufacturer's instructions. For assessment of lipid deposition, hearts were cryopreserved and whole-heart sections were stained with Oil Red O (Sigma-Aldrich) according to manufacturer's instructions.

2.6 Protein expression analysis

2.6.1 Western Blot

Postnatal day 1 hearts were harvested from mice. Tissues were homogenized with a pestle mortar mixer (3 rounds at 8 sec) in lysis buffer (10% NP40, 0.1 M EGTA, 0.5 M EDTA, 5M NaCl, 1M Tris HCl pH 7.5, ddH2O). Protein lysates were quantified using BCA protein assay. Protein lysates (10 ug) were prepared with 1X NuPAGE LDS sample buffer and 10% DTT and subsequently loaded as well as run on a 4-12% BOLT bis-tris gel. Proteins were transferred onto membranes at 220mA for 2 hours or 24 mA for 18 hours at 4º Celsius. Membranes were blocked in 5% milk in 1X TBST (1X TBS, 0.1% Tween) for 1 hour at room temperature. Membranes were incubated with primary antibodies (anti-DSP 1:1000, anti-PKP2 1:2000, anti-DSC2 1:1000, anti-JUP 1:1000, anti-N-cad 1:1000, anti-GAPDH 1:2000, anti-CX43 1:8000) at 4º Celsius with constant rocking. After primary incubation, blots were washed three times for 10 minutes with 1X TBST at room temperature with constant rocking. Secondary

antibody incubation (rabbit anti-mouse horseradish peroxidase, donkey anti-rabbit horseradish peroxidase) was performed at room temperature for 1 hour with constant rocking. Chemiluminescent substrates (SuperSignal West Dura Extended Duration substrate, SuperSignal West Femto Maximum Sensitivity substrate, and SuperSignal West Pico Chemiluminescent Substrate) were used at 1:1 ratio of peroxide and enhancer solutions to detect protein bands of interest.

2.6.2 Immunostaining

Mouse heart cryosections were fixed in 100% acetone for 8 minutes and subsequently washed twice with 1X PBS for 5 minutes. Cryosections were then permeabilized with 0.2% Triton X-100 for 10 minutes, blocked in 5% Donkey Serum in Gold Buffer (150 mM Tris-HCl, pH 8.0, 500 mM KCl) for 1 hour at room temperature then incubated with primary antibodies (anti-PKP2 (mouse, 1:100, Abcam) anti-N-Cad (rabbit, 1:10, Abcam)) in blocking buffer overnight at 4º Celsius. After primary incubation, sections were washed with 1X PBS three times for 5 minutes. Sections were subsequently stained with fluorescently labeled secondary antibodies (1:100, Alexa Fluor 488, mouse, Life Technologies) (Fluor 647, Rabbit, Jackson Laboratories) for 1 hour at room temperature then washed in 1X PBS three times for 10 minutes, followed by imaging using confocal microscopy (Olympus FV1000).

2.7 Neonatal Cardiomyocyte Isolation

Neonatal cardiomyocytes were prepared from 1 day old mice as previously described ((Lyon et al. 2014).

2.8 Cardiomyocyte Field Potential (electrophysiology)

Neonatal cardiomyocytes were plated at 40,000 cells per microelectrode recording well. Data acquisition is controlled by xCELLigence® RTCA CardioECR Data Acquisition software. Field potential (FP) data were collected at 0.1 ms (10 K Hz) with a bandwidth of 1 Hz to 3 KHz. Thirty minutes of baseline FP signals were taken by sampling cardiomyocytes every 5 minutes for 30 seconds. In order to analyze the complex electrical waves derived from neonatal cardiomyocytes FP responses, which is a measure of integrated ion channel activity, a number of parameters were derived. For analysis of FP signal, the FP spike amplitude (FPAmp) is derived, which is the absolute (delta) value in mV from lowest point of the initial spike to the highest point of the spike. The FP Duration (FPD) is defined as the time period between the negative peak of the FP spike to the maximum or minimum point of the reference wave. The reference wave can be negative or positive depending on how the cardiomyocytes are situated with respect to the FP electrodes. Raw data collected from ECR electrodes were analyzed offline using xCELLigence® RTCA CardioECR Data Analysis software. Positive peaks were automatically selected and beating rhythm irregularity was calculated as the coefficient of variation (standard deviation/average) of all positive peaks within the recording.

2.9. Statistical Analysis

Data presented in the text and figures are expressed as mean values ± SEM. Each study was replicated at least three times prior to statistical analysis. Significance was evaluated by two-tailed Student's t-test. For Kaplan-Meier survival analysis, significance was evaluated by the log-rank test. $P < 0.05$ was considered statistically significant.

Chapter 3

Adult PKP2 Homozygous Mutant Mice Recapitulate ARVC Disease Features

3.1 PKP2 c.2146-1G>C splice site equivalent mutation is sufficient to trigger classic disease features of ARVC in mice *in vivo*

Recent evidence highlights that altered RNA splicing may be a mechanism by which PKP2 genetics drives ARVC (Gerull et al. 2004; Groeneweg et al. 2014). PKP2 c.2146-1G>C mutation has been reported in multiple independent populations and thought to be pathogenic for ARVC due to clinical manifestations including sudden cardiac death, ventricular tachycardia, right and left bundle branch block, RV dilation and wall motion abnormality, and fibro-fatty replacement on wall biopsies (Gerull et al. 2004; Svensson et al. 2016; Syrris et al. 2006). To determine how the PKP2 c.2146-1G>C mutation recapitulates ARVC disease features, the Sheikh lab generated a CRISPR/Cas9 human equivalent PKP2 IVS10-1G>C mutation in the mouse (**Fig 1A**).

PKP2 Homozygous (Hom) mutant mice were viable at birth but selectively recapitulated all classic disease features of ARVC by 4 weeks of age. Sudden cardiac death is exhibited in PKP2 Hom mutant mice by 4 weeks of age, unlike PKP2 Heterozygous (Het) mutant and control mice (**Fig. 1B**). To determine whether PKP2 Hom mutant mice exhibit the classic electrical defects seen in ARVC patients, surface electrocardiogram recordings were performed at 4 weeks and showed no significant changes in heart rate, P wave duration, and PR interval, between PKP2 Hom mutant and control mice. However, the QRS interval was significantly prolonged in these mutant mice when compared to controls (**Fig. 1C**), suggesting ventricular depolarization delay. Furthermore, surface ECG recordings of 4-week old PKP2 Hom mutant mice indicate irregular cardiac rhythm and presence of ectopic beats (**Fig. 1C**). To determine the presence of ventricular remodeling, magnetic resonance imaging was performed, which showed right and left

ventricular dilation in PKP2 Hom mutant mice at 5 weeks (**Fig. 1D**), suggesting bi-ventricular dysfunction. To determine the whether PKP2 Hom mutant mouse hearts exhibit fibrofatty replacement of myocardium, Masson's trichrome staining and Oil Red O staining were performed. Representative Masson's trichrome stains demonstrated loss of myocardium and fibrotic tissue replacement with lipid deposition in the right ventricle, as highlighted by Oil Red O staining (**Fig. 1E**). These results highlighted that PKP2 Hom mutant mice exhibit all classic features of adult onset ARVC.

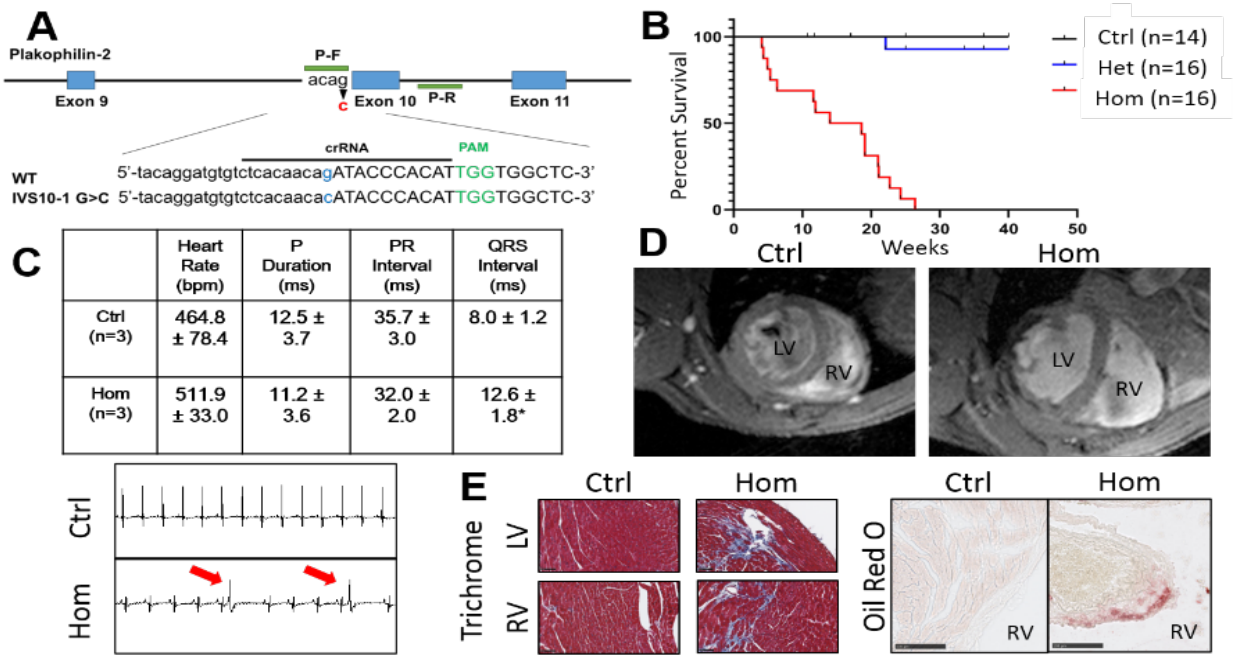

Figure 1: PKP2 Hom mutant mice display classic ARVC disease features. A. PKP2 genomic region for CRISPR/CAS9 strategy to generate PKP2 c.2146-1G>C mutation equivalent mice. **B.** Kaplan-Meier survival analysis of control (Ctrl), PKP2 heterozygous mutant (Het), and PKP2 homozygous mutant (Hom) mice. **C. (top)** Quantification of surface ECG parameters from Ctrl and PKP2 Hom mutant mice at 4 weeks of age. **C. (bottom)** Representative baseline surface ECG recordings from 4-week old Ctrl and PKP2 Hom mutant mice. Premature ventricular contractions are depicted with red arrows. **D.** Representative magnetic resonance images displaying both the left ventricle (LV) and right ventricle (RV) from 5-week old Ctrl and PKP2 Hom mutant mice. **E.** Masson's trichrome (left) and Oil Red O (right) stains of 6-week old Ctrl and PKP2 Hom mouse cardiac sections (Bradford WH., Unpublished Data, 2020).

Chapter 4

RNA and Protein Analysis of PKP2 IVS10-1G>C Mutation in Mouse Hearts

4.1 PKP2 IVS10-1G>C mutation causes partial intron retention that leads to a larger PKP2 transcript and mutant protein

RNA splice site mutations can have multiple consequences on RNA and protein quality. These can include: intron retention (larger product), exon skipping (shorter product), premature termination codon (no product) (Guernsey et al. 2010; Watanabe et al. 2013). In order to fully understand how the PKP2 IVS10-1G>C mutation manifests ARVC disease features in mice, it was critical to first understand how the mutation affected PKP2 RNA and encoded protein.

RNA analyses of adult PKP2 Hom mutant heart tissue using specific primers spanning exons 9 to 10 and encompassing the PKP2 mutation revealed a larger mutant PKP2 product (228 base pair (bp)), relative to endogenous wildtype (WT) PKP2 product **(**174 bp) observed in control hearts **(Fig. 2A).** Sequencing analyses of this larger transcript in PKP2 Hom mutant mouse heart identified that the mutant PKP2 retained a 54 bp intronic sequence **(Fig. 2B)**. Interestingly, RNA analyses of exons 11 to 13, which are outside the PKP2 mutation revealed PKP2 RNA transcripts at similar levels to wild type PKP2 **(Fig.2C)**, suggesting that total PKP2 RNA levels are not altered. At the protein level, PKP2 Hom mutant hearts express a higher molecular weight mutant PKP2 protein in the absence of endogenous PKP2 **(Fig. 2D)**, implying that either loss of wild type PKP2 or gain of mutant PKP2 protein mechanistically drives ARVC.

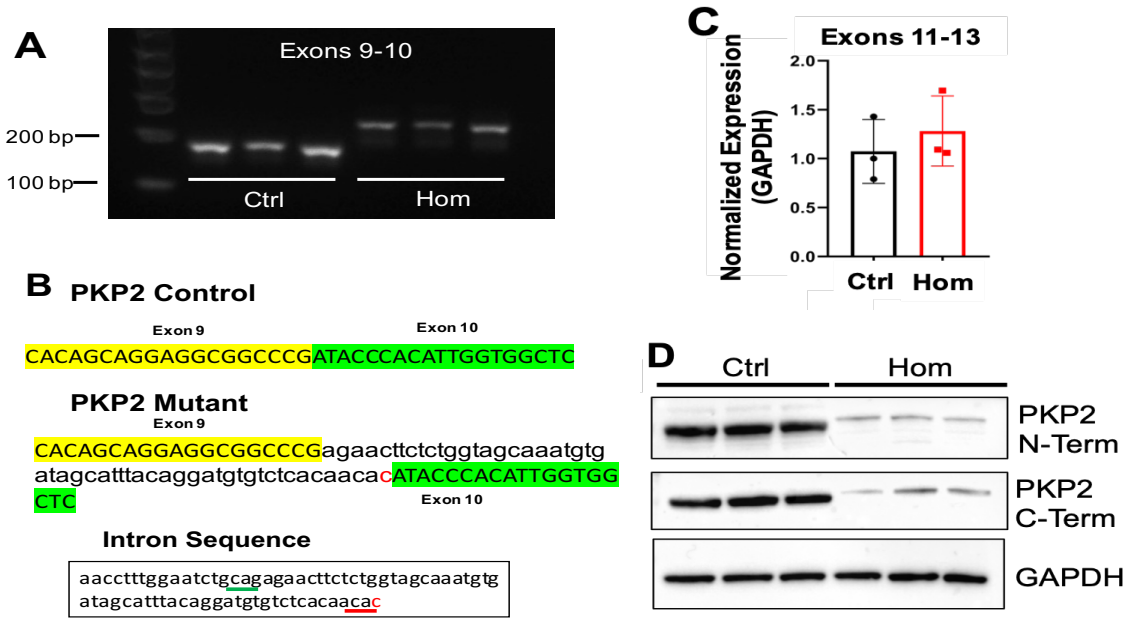

Figure 2: The PKP2 IVS10-1G>C mutation causes partial intron retention that leads to a larger PKP2 mutant protein. **A.** RT-PCR analysis of PKP2 exons 9 to 10 in mouse hearts. **B.** and sequencing analysis of products. PKP2 intron 9 sequence shows splice acceptor site (red) and an alternative upstream splice acceptor site (green). **C.** RT-qPCR analysis of PKP2 exons 11 to 13 in mouse hearts. **D.** PKP2 protein analysis using PKP2 N- and C-terminal antibodies in mouse hearts. Glyceraldehyde-3-Phosphate Dehydrogenase (GAPDH) is used as a loading control. (Bradford WH., Unpublished Data, 2020).

Chapter 5

Molecular Defects and Gross Morphology in Neonatal PKP2 Hom Mutant Mouse Hearts

5.1 PKP2 Hom mutant neonatal hearts provide insight into the early molecular pathways altered in ARVC

To determine the impact of the PKP2 RNA splice site mutation on PKP2 protein quality at early developmental stages of ARVC in the PKP2 Hom mutant model, we exploited neonatal PKP2 Hom (P1) mutant mice. Protein blot analyses of PKP2 Hom P1 mutant hearts showed the appearance of the larger molecular weight PKP2 in the absence of endogenous PKP2 and significant loss of desmosomal associated proteins (DSP, DSG2, JUP) (Fig. 3). The desmosomal disruption in PKP2 P1 mutant hearts was observed in the absence of disruption of fascia adherens (mechanical) junction protein (N-Cad) and gap junction protein (Cx43), when compared to controls (**Fig. 3**). Immunofluorescence imaging analyses further revealed that the mutant PKP2 protein retained intact junctional localization as shown by its co-localization with the fascia adherens junctional marker, N-cadherin, similar to controls that contains endogenous PKP2 **(Fig. 4)**. Although microscopy is not a quantitative assay, an obvious decrease in PKP2 intensity could be observed in PKP2 mutant hearts, further validating findings from protein blot analyses. The desmosomal protein defects were observed in PKP2 Hom mutant hearts was observed in the absence of overt cardiac disease, as no significant differences in heart weight to body weight (HW/BW) ratios were observed when compared to controls **(Fig. 5A)**. RNA analyses further demonstrated no significant differences in the expression of cardiac stress marker genes, atrial natriuretic factor (ANF) and B-type natriuretic factor (BNP), as well as pro-fibrotic genes, collagen α1 types I (Col1a1) and III (Col3a1) when compared to controls. **(Fig. 5B, Fig 5C)**, highlighting the specificity of the PKP2 RNA splice site mutation to primarily impact PKP2 protein quality and desmosomal interactions as well as provide insight into the early molecular pathways that are likely triggers for the late stage structural disease.

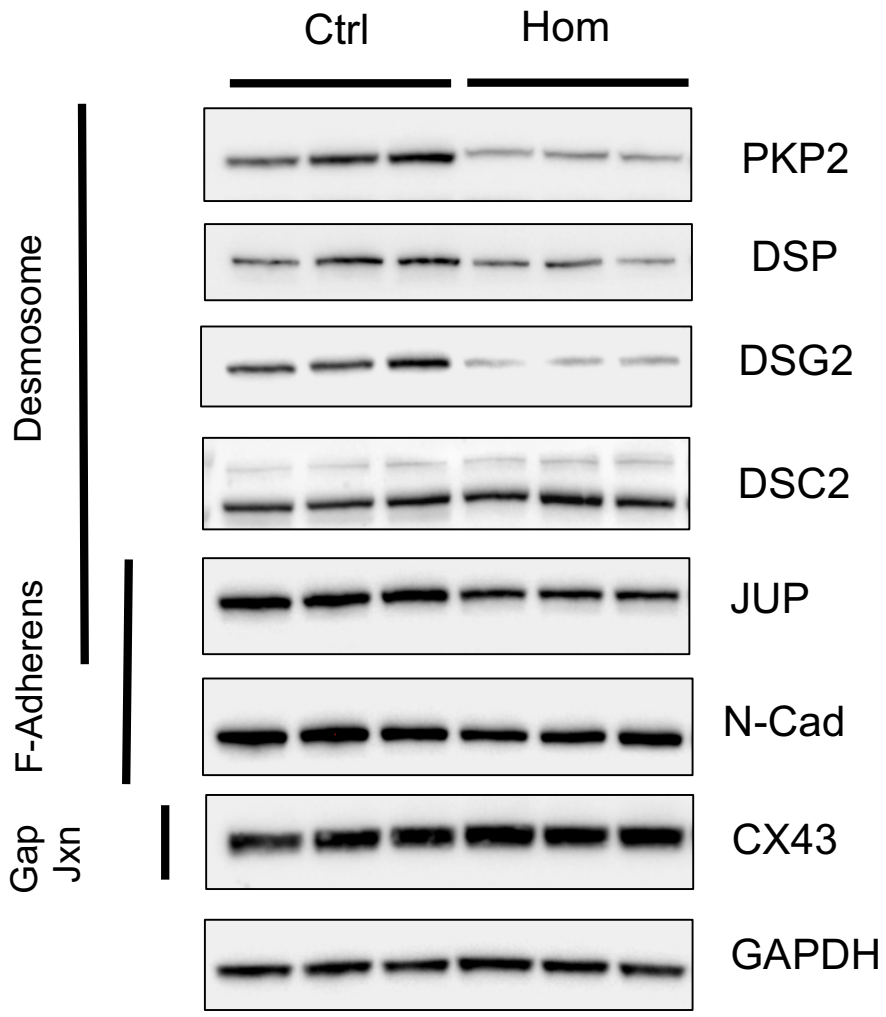

Figure 3: **PKP2 Hom mutant neonatal mouse hearts display desmosomal defects**. Protein blot analysis of desmosomal (PKP2, DSP, DSG2, JUP), fascia adherens junction (JUP, N-Cad) and gap junction (CX43) markers in neonatal hearts. GAPDH is a loading control.

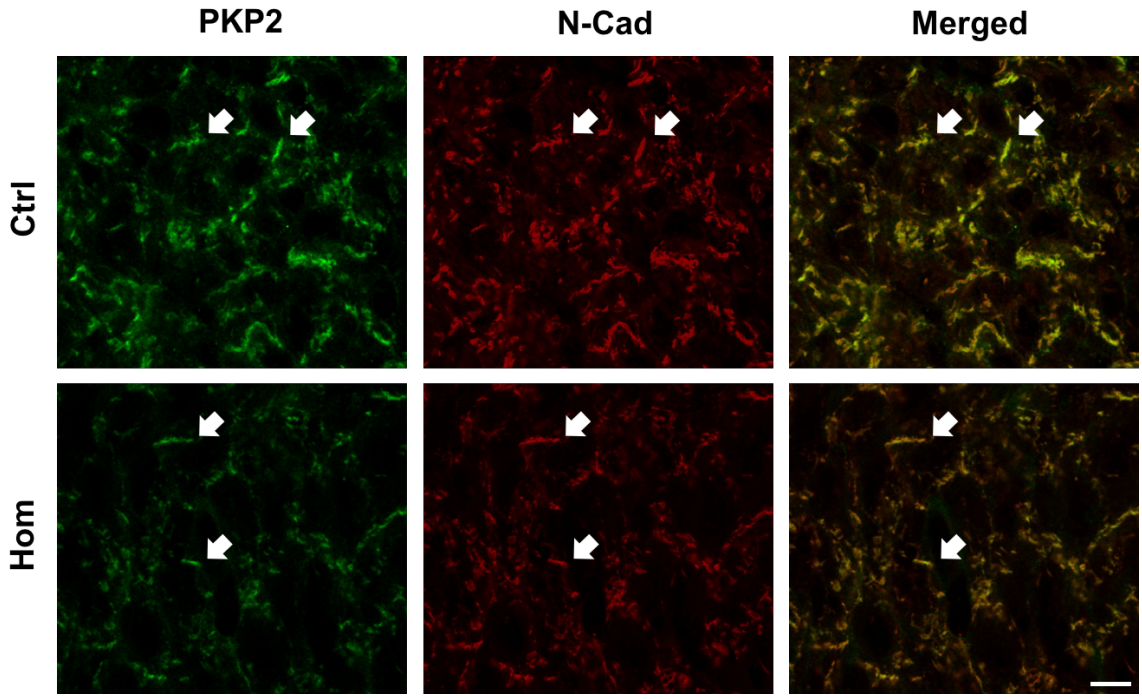

Figure 4: Mutant PKP2 protein retains junctional localization in neonatal mouse hearts. Representative immunofluorescence microscopy images of plakophilin-2 (PKP2) and N-cadherin (N-Cad) expression in control (Ctrl) and PKP2 Hom (Hom) mutant neonatal mouse hearts. Arrows highlight co-localization between PKP2 and N-Cad stains.

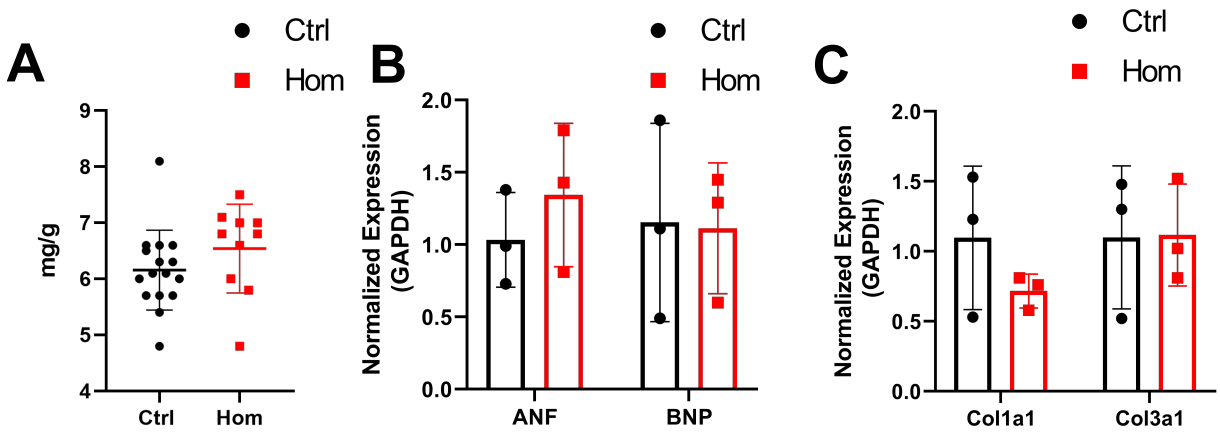

Figure 5: Absence of gross morphological changes and overt cardiac disease in PKP2 P1 Hom Mutant Mice. A. P1 Heart weight to body weight ratios (HW/BW). **B.** RT-qPCR of cardiac stress markers atrial natriuretic factor (ANF) and B-type natriuretic factor (BNP), and **C.** profibrotic genes collagen α1 types I (Col1a1) and III (Col3a1) in P1 hearts.

Chapter 6

Molecular and Cellular Defects in Neonatal PKP2 Hom Mutant Cardiomyocytes

6.1 PKP2 Hom mutant neonatal cardiomyocytes exhibit desmosomal disruption, which prime cardiomyocytes to frequent baseline arrhythmias

Mechanisms explaining ARVC disease features implicate a direct link to disruption of cardiomyocytes (Romero et al. 2013; Zhou and Pu 2016). To determine the primary effects of PKP2 IVS10-1G>C mutation in cardiomyocytes, we sought to assess the effects on PKP2 protein quality in neonatal PKP2 Hom (P1) mutant cardiomyocytes. Similar to neonatal PKP2 mutant hearts, protein blot analyses of PKP2 Hom mutant neonatal cardiomyocytes showed the appearance of a higher molecular weight mutant PKP2 protein, in the absence endogenous PKP2 protein **(Fig. 6).** These defects in PKP2 protein quality in PKP2 Hom mutant cardiomyocytes led to a significant and specific disruption in desmosomal protein complexes (DSP, DSG2, JUP) in the absence of changes to other mechanical junction components (N-Cad) and gap junction components (Cx43) **(Fig. 6)**.

Ventricular arrhythmias, such as premature ventricular contractions and ventricular extra-systoles, are some of the classic early cardiomyocyte disease features observed in ARVC patients (Sen-Chowdhry et al. 2010). To determine the functional effects of the PKP2 RNA splice site mutation (IVS10-1G>C) *in vitro*, electrophysiological activity was monitored in PKP2 Hom mutant neonatal cardiomyocytes using field potential (electrical activity surrogate) in the xCELLigence® RTCA CardioECR system. Aggregate electrical field potentials were recorded and analysis of baseline electrical firing of PKP2 Hom neonatal cardiomyocytes revealed significant rhythm irregularity (arrhythmias) (**Fig 7.)**. These studies altogether highlight the specificity of the PKP2 RNA splice site mutation to primarily impact PKP2 protein quality and desmosomal interactions, which predispose cardiomyocytes to baseline arrhythmias.

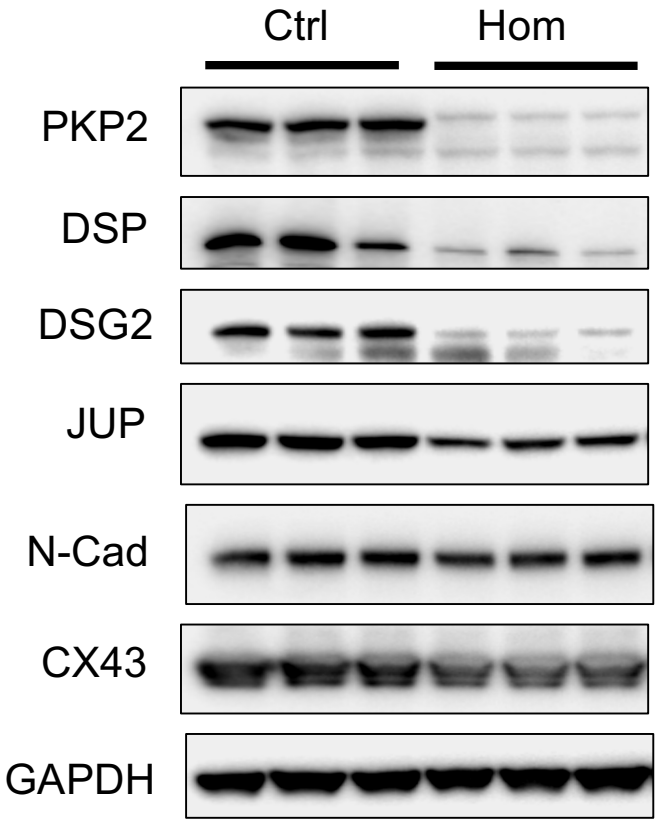

Figure 6: PKP2 Hom neonatal cardiomyocytes display desmosomal defects. Protein blot analysis of desmosomal (PKP2, DSP, DSG2, JUP), fascia adherens junction (JUP, N-Cad) and gap junction (CX43) markers in neonatal cardiomyocytes. GAPDH is used as a loading control.

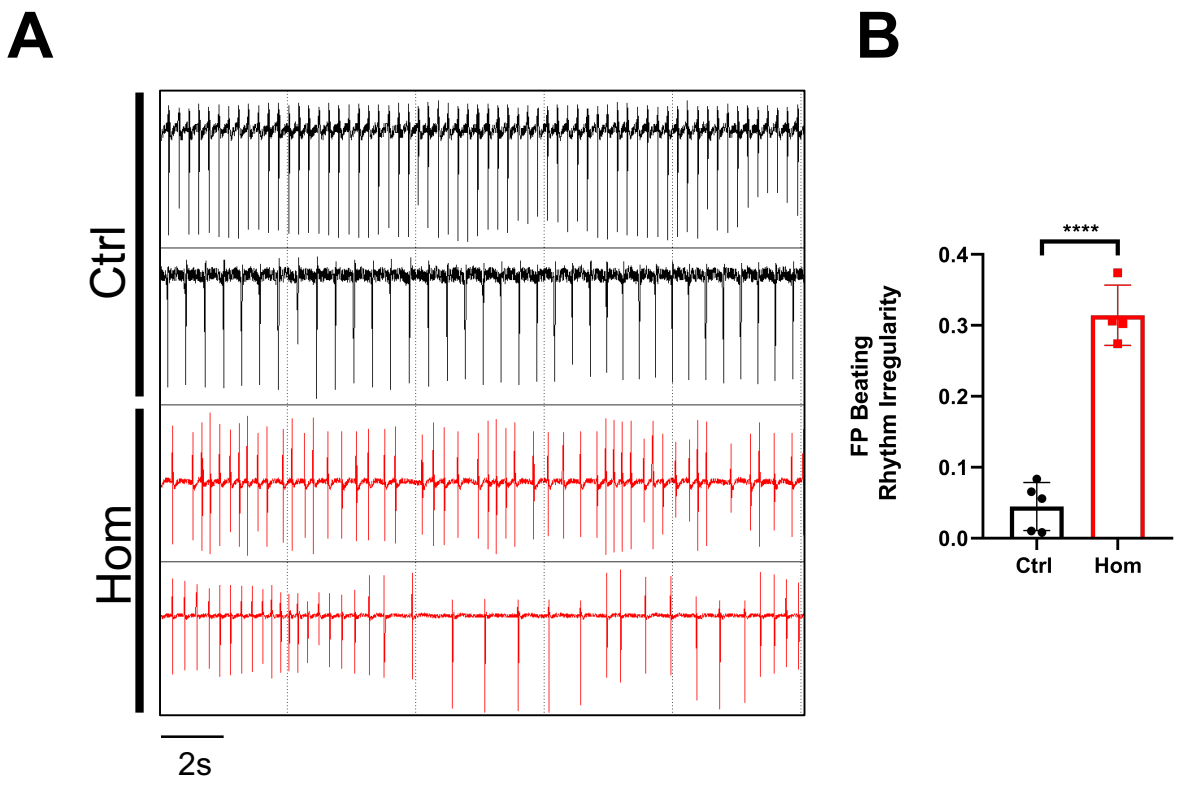

Figure 7: PKP2 Hom mutant neonatal cardiomyocytes exhibit baseline arrhythmias. A. Representative field potential (FP) tracings from two independent wells. Bar represents 2 seconds of time. **B.** FP beating rhythm irregularity index in neonatal cardiomyocytes from two independent wells within five independent experiments. ****, $p<0.0001$.

Chapter 7

Discussion

7.1 Discussion

There are limited mouse models harboring PKP2 genetics that fully recapitulate ARVC disease features. Additionally, these models provide little insight into the early development of ARVC. These studies provide evidence for the role of a prevalent PKP2 patient mutation (c.2146-1G>C), which we show is sufficient to recapitulate all adult onset disease features associated with ARVC. Based on the characterization of this novel mouse model, my thesis studies provide insights into early ARVC disease stages in this model, to mine for early-disease driving pathways underlying ARVC.

7.1.1 PKP2 RNA splicing impacts PKP2 protein quality which drives ARVC

In vivo studies in PKP2 Hom mutant mice have further elucidated the effects of PKP2 RNA splicing on PKP2 protein quality, which we show is a driving factor in triggering all classic disease features associated with adult onset-ARVC. These classic ARVC disease features included (i) ventricular arrhythmias, such as prolonged QRS intervals and the presence of ventricular ectopic beats, (ii) ventricular dysfunction as evidenced by MR images indicating biventricular dilation, (iii) loss of myocardium and replacement fibrosis and lipid/fat deposits, as highlighted by Masson's trichrome and Oil Red O staining, and (iv) premature death by 4 weeks of age, reminiscent of sudden cardiac death observed in ARVC. These findings add to the field by providing RNA splicing defects as a novel mechanism that is sufficient to disrupt desmosomal protein quality and trigger ARVC, while also providing a novel mouse model harboring PKP2 genetics that can recapitulate the full spectrum of ARVC.

7.1.2 PKP2 protein quality impacts specific interactions at the desmosome

At the mechanistic level, either loss of endogenous PKP2 and gain of mutant PKP2 are factors driving the full spectrum of ARVC. PKP2 is a critical protein to the structure and functioning of the desmosome (Bass-Zubek et al. 2008). *In vivo* and *in vitro* studies in neonatal PKP2 Hom mutant mice and cardiomyocytes, respectively, highlight the early and selective desmosomal disruption that are triggers for late stage ARVC disease. Current genetic mouse models harboring loss of PKP2 or overexpression of mutant PKP2 provide limited insights into the early impact on desmosomal protein levels and quality in cardiac development in mice *in vivo*. For example, within the PKP2 heterozygous knockout model, only selective effects on JUP protein levels were assessed in adult mouse hearts and no significant difference was observed in its expression when compared to controls (Cerrone et al. 2012). Studies in cardiomyocyte-specific, inducible, PKP2 knockout mice also did not comprehensively assess cell-cell junction proteins (Cerrone et al. 2017). Moreover, global PKP2 knockout mouse model observed disruption to some desmosomal markers (DSP, JUP) but no significant decrease was observed in DSG2 in embryonic mouse hearts (Grossmann et al. 2004), validating findings in our PKP2 Hom mutant mouse model, which also harbor loss of endogenous PKP2 and the early onset of desmosomal disruption (albeit DSG2 was also impacted). Interestingly, embryonic loss of PKP2 resulted in early embryonic lethality (Grossmann et al. 2004); however, our PKP2 Hom mutant mice also harbor loss of endogenous PKP2 yet are viable at birth, suggesting a potential role for compensation by the larger mutant PKP2 in embryonic survival in our PKP2 Hom mutant mice. Studies overexpressing mutant PKP2 in mice revealed a hierarchy of desmosomal protein loss that may be distinct as endogenous PKP2 remained (albeit reduced) in these models. For example, cardiac-specific overexpression of PKP2 S239X mutant (resulting in a truncated form

of PKP2) in mice resulted in a significant decrease in endogenous PKP2, JUP, and β-cat in adult mouse hearts that expressed high levels of the transgene (Moncayo-Arlandi et al. 2016). Interestingly, DSP and DSC2 protein expression were not changed in adult PKP2 S239X mutant mouse hearts, and these molecular defects correlated with mice surviving up to 12 months of age (Moncayo-Arlandi et al. 2016). Another study overexpressing a PKP2 R735X mutant (resulting in a truncated form of PKP2) in adult mice revealed intact PKP2 and JUP localization but altered CX43 localization, despite normal protein and mRNA expression levels (Cruz et al. 2015)., thus highlighting limited impacts of mutant PKP2 at cell-cell junctions. These studies altogether reveal that the presence of endogenous PKP2 may provide a "graded or limited response" to the impact of the PKP2 mutant on adult cardiac desmosomal protein quality and integrity as well as survival. Interestingly, PKP2 Hom mutant mice exhibited premature death by 4 weeks of age, providing a unique opportunity to observe the impact of mutant PKP2 in the absence of endogenous PKP2 in the developing heart, and the sufficiency of these molecular alterations to drive premature death in adult mice. Thus, our studies add to the field by showing how a prevalent PKP2 splice site mutation impacts RNA splicing and desmosomal protein quality (evidenced by molecular disruption of the desmosome) at an early stage. Additionally, these studies help elucidate how a combination of loss of endogenous PKP2 and gain of mutant PKP2 may be a driving factor in ARVC disease progression. PKP2 Hom mutant mice, also further highlight the consequence of the splice site mutation on desmosomal interactions (PKP2, DSP, DSG2, JUP) in neonatal stages, in heart tissue and cardiomyocytes, in the absence of overt structural disease.

7.1.3 Early drivers of ARVC

Electrical defects are a primary and driving feature of ARVC (Andrews et al. 2017; Cerrone et al. 2012; Sen-Chowdhry et al. 2010)). *In vivo* studies utilizing PKP2 Hom mutant neonatal cardiomyocytes demonstrate a role for loss of endogenous PKP2 and appearance of mutant PKP2 in driving early baseline arrhythmias. The studies in this thesis are consistent with studies in some other PKP2 genetic models, such as PKP2 global heterozygous knockout mice which harbored ventricular arrhythmias as the primary disease feature observed (Cerrone et al. 2012). Previous studies have given insight into many molecular players driving a connection between desmosomal proteins and electrical dysfunction. Abnormal electrical activity attributed to Cx43 loss has been observed in studies exploiting DSP deficient neonatal cardiomyocytes and mice, suggesting Cx43 loss may trigger the cardiac arrhythmias underlying ARVC (Lyon et al. 2014). A reduction in PKP2 expression via the use of shRNA silencing in neonatal rat ventricular myocytes also resulted in a decrease in total Cx43 content and a significant redistribution of Cx43 to the intracellular space, leading to significant reduction in sodium current (Cerrone et al. 2012). However, neonatal PKP2 Hom mutant neonatal mouse hearts and cardiomyocytes showed no impact on Cx43 expression, yet baseline arrhythmias were observed. Recent studies, implicate new pathways associated with the electrical dysfunction associated with PKP2 deficiency/mutations. Although baseline arrhythmias were not observed in cardiac-inducible loss of PKP2 in adult ventricular myocytes (only isoproterenol-induced arrhythmias), these studies revealed reduction in the expression of critical proteins involved in intracellular calcium homoeostasis (ryanodine receptor 2 (RyR2), ankyrin-B, calcium channel, voltage-dependent, L type, alpha 1C subunit (CaV1.2), and triadin) in hearts of these mice (Cerrone et al. 2017), highlighting molecular pathways that may predispose to arrhythmias. Further studies into

assessing the expression of calcium handling pathways may help better understand the appearance of arrhythmias in PKP2 Hom neonatal cardiomyocytes. This thesis has established an *in vitro* PKP2 based model that can be used to mine the early pro-arrhythmogenic pathways (eg. calcium handling pathways) that may drive the electrical defects during the clinically concealed phase of ARVC in the absence of overt structural disease.

7.2 Conclusions

In conclusion, by exploiting CRISPR-Cas9 based genomic engineering approaches to generate a novel knock-in mouse model harboring a prevalent human PKP2 (c.2146-1G>C) splice site mutation, we have highlighted the sufficiency of PKP2 RNA splicing to recapitulate all of the classic features associated with ARVC, thus providing a unique model system to study the impact of PKP2 patient genetics in ARVC. We further highlight that the neonatal stage in PKP2 Hom mutant mice provides a developmental window that can be exploited to observe primary molecular, cellular and physiological defects that are associated with early ARVC disease as well as platform to test therapeutic approaches to reverse early disease. These results are timely as PKP2 is the most frequently mutated gene in ARVC, yet there are limited efforts in understanding the early drivers and consequences of the disease in these patients. Using this novel PKP2 mutant mouse model, key molecular features indicated by loss of endogenous PKP2 and other desmosomal proteins alongside appearance of a larger molecular weight mutant PKP2 have been discovered. Additionally, we observed arrhythmias in heart muscle cells of PKP2 mutant mice that precede the gross structural destruction of the heart that occurs at late stages.

7.3 Future Studies

These studies characterize a stage in a mouse model of ARVC that is an ideal time point to help elucidate the mechanisms of how the PKP2 genetics/splice site mutations drive ARVC disease progression, as well as platform for new therapeutics. Further insight into the mechanistic understanding of whether the loss of endogenous PKP2 or appearance of mutant PKP2 protein drives ARVC disease features in vitro and in vivo can be assessed using an adenoviral and AAV approaches, respectively. An adenoviral and AAV targeted delivery approach of PKP2 wildtype and mutant protein in neonatal cardiomyocytes and neonates, respectively, can be used to help determine whether mutant PKP2 protein exacerbates disease features by protein toxicity or rescues due to protein stability, as well as whether restoration of wild type PKP2 is sufficient to rescue ARVC disease features. Additionally, in depth RNA sequencing analyses could be used to provide an overview of the altered gene expression patterns observed in PKP2 Hom mutant hearts, and would provide insight new molecular pathways targeted by the RNA splice site mutation and identify novel markers that define ARVC in desmosomal genes impacted by RNA splicing. Furthermore, recent precision based (prime editor) genome editing approaches have highlighted new avenues to correct/repair gene mutations (Anzalone et al. 2019). Using a catalytically impaired Cas9 endonuclease fused to an engineered reverse transcriptase, this new approach re-writes new genetic information into a specified DNA site (Anzalone et al. 2019). The PKP2 Hom mutant model provides an ideal platform to test these genome repair approaches as a potential editing approach for correcting the PKP2 mutations, that may also be translated to mutations in other human genetic based diseases.

References

Andrews, Christopher M. 2017. "The Electrical and Structural Substrate of Arrhythmogenic Right Ventricular Cardiomyopathy Determined Using Noninvasive Electrocardiographic Imaging and Late Gadolinium Magnetic Resonance Imaging." *Circulation. Arrhythmia and electrophysiology* 10(7). https://www.ncbi.nlm.nih.gov/pmc/articles/PMC5533087/ (May 20, 2020).

Anna, Abramowicz, and Gos Monika. 2018. "Splicing Mutations in Human Genetic Disorders: Examples, Detection, and Confirmation." *Journal of Applied Genetics* 59(3): 253–68.

Anzalone, Andrew V. 2019. "Search-and-Replace Genome Editing without Double-Strand Breaks or Donor DNA." *Nature* 576(7785): 149–57.

Bass-Zubek, Amanda E. 2008. "Plakophilin 2: A Critical Scaffold for PKC Alpha That Regulates Intercellular Junction Assembly." *The Journal of Cell Biology* 181(4): 605–13.

Baumgart, Ann-Kathrin, and Marc Beyer. 2017. "Genetic Engineering as a Tool for the Generation of Mouse Models to Understand Disease Phenotypes and Gene Function." *Current Opinion in Biotechnology* 48: 228–33.

Bradford, William H. 2020. *Mechanistic Insights into RNA Splicing as a Trigger for Arrhythmogenic Right Ventricular Cardiomyopathy* [Unpublished manuscript]. Department of Medicine, University of California-San Diego, La Jolla, California.

Carrier, Lucie, Giulia Mearini, Konstantina Stathopoulou, and Friederike Cuello. 2015. "Cardiac Myosin-Binding Protein C (MYBPC3) in Cardiac Pathophysiology." *Gene* 573(2): 188–97.

Carvajal-Huerta, L. 1998. "Epidermolytic Palmoplantar Keratoderma with Woolly Hair and Dilated Cardiomyopathy." *Journal of the American Academy of Dermatology* 39(3): 418–21.

Cerrone, Marina. 2012. "Sodium Current Deficit and Arrhythmogenesis in a Murine Model of Plakophilin-2 Haploinsufficiency." *Cardiovascular Research* 95(4): 460–68.

Cerrone, Marina. 2017. "Plakophilin-2 Is Required for Transcription of Genes That Control Calcium Cycling and Cardiac Rhythm." *Nature Communications* 8(1): 106.

Cho, Yongkeun. 2018. "Arrhythmogenic Right Ventricular Cardiomyopathy." *Journal of Arrhythmia* 34(4): 356–68.

Corrado, Domenico. 2003. "Does Sports Activity Enhance the Risk of Sudden Death in Adolescents and Young Adults?" *Journal of the American College of Cardiology* 42(11): 1959–63.

Cruz, Francisco M. 2015. "Exercise Triggers ARVC Phenotype in Mice Expressing a Disease-Causing Mutated Version of Human Plakophilin-2." *Journal of the American College of Cardiology* 65(14): 1438–50.

Dalal, Darshan. 2005. "Arrhythmogenic Right Ventricular Dysplasia: A United States Experience." *Circulation* 112(25): 3823–32.

DeBry, Ronald W., and Michael F. Seldin. 1996. "Human/Mouse Homology Relationships." *Genomics* 33(3): 337–51.

Gerull, Brenda. 2004. "Mutations in the Desmosomal Protein Plakophilin-2 Are Common in Arrhythmogenic Right Ventricular Cardiomyopathy." *Nature Genetics* 36(11): 1162–64.

Groeneweg, Judith A. 2014. "Functional Assessment of Potential Splice Site Variants in Arrhythmogenic Right Ventricular Dysplasia/Cardiomyopathy." *Heart Rhythm* 11(11): 2010–17.

Grossmann, Katja S. 2004. "Requirement of Plakophilin 2 for Heart Morphogenesis and Cardiac Junction Formation." *The Journal of Cell Biology* 167(1): 149–60.

Guernsey, Duane L. 2010. "Mutation in the Gene Encoding Ubiquitin Ligase LRSAM1 in Patients with Charcot-Marie-Tooth Disease." *PLoS genetics* 6(8).

Kathiresan, Sekar, and Deepak Srivastava. 2012. "Genetics of Human Cardiovascular Disease." *Cell* 148(6): 1242–57.

Lim, Kian Huat. 2011. "Using Positional Distribution to Identify Splicing Elements and Predict Pre-MRNA Processing Defects in Human Genes." *Proceedings of the National Academy of Sciences of the United States of America* 108(27): 11093–98.

Lyon, Robert C. 2014. "Connexin Defects Underlie Arrhythmogenic Right Ventricular Cardiomyopathy in a Novel Mouse Model." *Human Molecular Genetics* 23(5): 1134–50.

Marcus, Frank I., Sue Edson, and Jeffrey A. Towbin. 2013. "Genetics of Arrhythmogenic Right Ventricular Cardiomyopathy: A Practical Guide for Physicians." *Journal of the American College of Cardiology* 61(19): 1945–48.

Moncayo-Arlandi, Javier. 2016. "Molecular Disturbance Underlies to Arrhythmogenic Cardiomyopathy Induced by Transgene Content, Age and Exercise in a Truncated PKP2 Mouse Model." *Human Molecular Genetics* 25(17): 3676–88.

Mozaffarian Dariush. 2016. "Executive Summary: Heart Disease and Stroke Statistics—2016 Update." *Circulation* 133(4): 447–54.

Norgett, Elizabeth E. 2000. "Recessive Mutation in Desmoplakin Disrupts Desmoplakin–Intermediate Filament Interactions and Causes Dilated Cardiomyopathy, Woolly Hair and Keratoderma." *Human Molecular Genetics* 9(18): 2761–66.

Ohno, Seiko. 2016. “The Genetic Background of Arrhythmogenic Right Ventricular Cardiomyopathy.” *Journal of Arrhythmia* 32(5): 398–403.

Rampazzo, Alessandra. 2002. “Mutation in Human Desmoplakin Domain Binding to Plakoglobin Causes a Dominant Form of Arrhythmogenic Right Ventricular Cardiomyopathy.” *American Journal of Human Genetics* 71(5): 1200–1206.

Romero, Jorge, Eliany Mejia-Lopez, Carlos Manrique, and Richard Lucariello. 2013. “Arrhythmogenic Right Ventricular Cardiomyopathy (ARVC/D): A Systematic Literature Review.” *Clinical Medicine Insights. Cardiology* 7: 97–114.

Sen-Chowdhry, Srijita, Robert D. Morgan, John C. Chambers, and William J. McKenna. 2010. “Arrhythmogenic Cardiomyopathy: Etiology, Diagnosis, and Treatment.” *Annual Review of Medicine* 61: 233–53.

Sheikh, Farah, Robert S. Ross, and Ju Chen. 2009. “Cell-Cell Connection to Cardiac Disease.” *Trends in Cardiovascular Medicine* 19(6): 182–90.

Simpson, M. A. 2009. “Homozygous Mutation of Desmocollin-2 in Arrhythmogenic Right Ventricular Cardiomyopathy with Mild Palmoplantar Keratoderma and Woolly Hair.” *Cardiology* 113(1): 28–34.

Svensson, Anneli. 2016. “Arrhythmogenic Right Ventricular Cardiomyopathy - 4 Swedish Families with an Associated PKP2 c.2146-1G>C Variant.” *American Journal of Cardiovascular Disease* 6(2): 55–65.

Syrris, Petros. 2006. “Clinical Expression of Plakophilin-2 Mutations in Familial Arrhythmogenic Right Ventricular Cardiomyopathy.” *Circulation* 113(3): 356–64.

Tabib, A. 2003. “Circumstances of Death and Gross and Microscopic Observations in a Series of 200 Cases of Sudden Death Associated with Arrhythmogenic Right Ventricular Cardiomyopathy and/or Dysplasia.” *Circulation* 108(24): 3000–3005.

Te Riele, Anneline S. J. M. 2012. “Genotype-Specific Pattern of LV Involvement in ARVD/C.” *JACC. Cardiovascular imaging* 5(8): 849–51.

Thiene, Gaetano, Domenico Corrado, and Cristina Basso. 2007. “Arrhythmogenic Right Ventricular Cardiomyopathy/Dysplasia.” *Orphanet Journal of Rare Diseases* 2(1): 1–16.

Vermij, Sarah H., Hugues Abriel, and Toon A. B. van Veen. 2017. “Refining the Molecular Organization of the Cardiac Intercalated Disc.” *Cardiovascular Research* 113(3): 259–75.

Watanabe, Tohru. 2013. “A Mutant MRNA Expression in an Endomyocardial Biopsy Sample Obtained from a Patient with a Cardiac Variant of Fabry Disease Caused by a Novel Acceptor Splice Site Mutation in the Invariant AG of Intron 5 of the α-Galactosidase A Gene.” *Internal Medicine (Tokyo, Japan)* 52(7): 777–80.

Yadav, Sunil, Yoel H. Sitbon, Katarzyna Kazmierczak, and Danuta Szczesna-Cordary. 2019. "Hereditary Heart Disease: Pathophysiology, Clinical Presentation, and Animal Models of HCM, RCM, and DCM Associated with Mutations in Cardiac Myosin Light Chains." *Pflugers Archiv: European Journal of Physiology* 471(5): 683–99.

Zhang, Qing. 2018. "Mutations in Voltage-Gated L-Type Calcium Channel: Implications in Cardiac Arrhythmia." *Channels (Austin, Tex.)* 12(1): 201–18.

Zhou, Pingzhu, and William T. Pu. 2016. "Recounting Cardiac Cellular Composition." *Circulation research* 118(3): 368–70.